OAK RIDGE
NATIONAL LABORATORY

MANAGED BY UT-BATTELLE
FOR THE DEPARTMENT OF ENERGY

ORNL/TM-2001/235

Preliminary Results of Testing of Flow Effects on Evaporator Scaling

M. Z. Hu
D. W. DePaoli
D. T. Bostick'
C. Tsouris
A. B. Walker

UT-BATTELLE
ORNL-27 (4-00)

ORNL/TM-2001/235

Nuclear Science and Technology Division

Preliminary Results of Testing of Flow Effects on Evaporator Scaling

M. Z. Hu
D. W. DePaoli
D. T. Bostick
C. Tsouris
A. B. Walker

Date Published: February 2002

Prepared by
OAK RIDGE NATIONAL LABORATORY
Oak Ridge, Tennessee 3783 l-6285
managed by
UT-BATTELLE, LLC
for the
U.S. Department of Energy
under contract DE-AC05-00OR22725

CONTENTS

EXECUTIVE SUMMARY

This investigation has focused on the effects of fluid flow on solids deposition from solutions that simulate the feed to the 2H evaporator at the Savannah River Site. Literature studies indicate that the fluid flow (or shear) affects particle-particle and particle-surface interactions and thus the phenomena of particle aggregation in solution and particle deposition (i.e., scale formation) onto solid surfaces. Experimental tests were conducted with two configurations: (1) using a rheometer to provide controlled shear conditions and (2) using controlled flow of reactive solution through samples of stainless steel tubing. All tests were conducted at 80°C and at high silicon and aluminum concentrations, 0.133 *M* each, in solutions containing 4 *M* sodium hydroxide and 1 A4 each of sodium nitrate and sodium nitrite.

Two findings from these experiments are important for consideration in developing approaches for reducing or eliminating evaporator scaling problems:

- The rheometer tests suggested that for the conditions studied, maximum solids deposition occurs at a moderate shear rate, approximately 12 s^{-1}. That value is expected to be on the order of shear rates that will occur in various parts of the evaporator system; for instance, a 6 gal/min single-phase liquid flow through the 2-in. lift or gravity drain lines would result in a shear rate of approximately 16 s^{-1}. These results imply that engineering approaches aimed at reducing deposits through increased mixing would need to generate shear near all surfaces significantly greater than 12 s^{-1}. However, further testing is needed to set a target value for shear that is applicable to evaporator operation. This is because the measured trend is not statistically significant at the 95% confidence interval due to variability in the results. In addition, testing at higher temperatures and lower concentrations of aluminum and silicon would more accurately represent conditions in the evaporator. Without further testing, it does not appear advisable to depend on increased agitation as the primary means for reduction of scale in the 2H evaporator.

- The tubes used in the flow tests became clogged with solids when the solutions were below 80°C at the start of the test; a very striking difference from experiments with fully preheated solutions, which yielded only thin films of solids on the tubes. These results suggest that significant differences are found in the "stickiness" of solids formed at different temperatures. This may provide opportunities for engineering approaches to reduce solids deposition, such as feed dispersion or feed preheating. It is recommended that further studies be undertaken to determine what forms of sodium aluminosilicates adhere to stainless steel surfaces, under what conditions these materials are created, and what changes in evaporator operation could be made to minimize their formation.

1. INTRODUCTION

The processes of crystallization and solid deposit formation that led to the shutdown of 2H evaporator operations at the Savannah River Site (SRS) and that could possibly cause similar problems or in other evaporators must be made fully understood. During Phase I studies for FY 2001, we used dynamic light scattering to collect dynamic particle growth data; conducted solid-layer deposition tests under various temperatures, concentrations of silicon, and aluminum; and obtained preliminary findings in regard to the fluid-flow effect on the solid deposition on stainless steel surfaces. Results of this work are summarized in the report *Dynamic Particle Growth Testing – Phase I Studies.'*

The dynamic particle growth results, along with those from other testing and thermodynamic modeling, were presented to a review panel at a workshop at SRS on June 6, 2001. The technical experts concluded that with current and expected feed compositions, solids buildup in the evaporators may continue under certain conditions. They recommended that bench-scale testing be conducted to determine operating and design changes that could increase the time between evaporator cleanings. Among the higher-priority recommendations for experimentation, the consultants identified agitating the evaporator pot, dispersing the feed, and adding seed particles and/or adding a premix tank for aging the feed and forming particles under more-controlled conditions. The work described in this report was based upon those recommendations and involved simple tests that focus on clarifying the effects of fluid flow on deposition. The report presents results obtained to date in testing of solids formation and deposition in two configurations: (1) using a rheometer to provide controlled shear conditions and (2) using controlled flow of reactive solution through samples of stainless steel tubing.

2. OBJECTIVE

The experiments that were undertaken are part of testing designed to investigate how process parameters and engineering strategies affect the deposition of solids on stainless steel surfaces. The tests were aimed at understanding the effects of fluid-flow batch systems, and specifically at measuring what levels of velocity/shear and/or seeding are required to reduce or eliminate deposition of solids. The results of these studies will aid the development of engineering strategies to mitigate solid scale formation on surfaces in evaporator systems. The work was focused on providing the following benefits to plant operations:

- Confirm the importance of fluid flow on solids deposition, a finding that was suggested in previous tests.
- Identify a target level for local energy dissipation and/or fluid velocity in the evaporator. Further work will be necessary to translate this knowledge to set the lance flow rate and to guide any other efforts to increase mixing.
- Identify target levels for shear/velocity for flow in tubes, which relates to flow rates in the lift and gravity drain lines. This information will provide an estimate for the minimum lift rate needed to avoid line plugging.

3. BACKGROUND

3.1 OBSERVATIONS FROM PREVIOUS TESTING

Testing in multiple tasks related to solids deposition in the SRS 2H evaporator have indicated that fluid-flow patterns may have a significant effect on the nature and quantity of sodium aluminosilicate solids deposited on metal surfaces. Batch testing conducted by Mattus et al.,[2] Rosencrance et al.,[3] and Addai-Mensah[4] found similar overall trends on the effect of fluid flow on solids deposition in stirred tanks. Their results showed that, walls of vessels that were operated at a higher rate of mixing, or at a greater energy dissipation rate had smaller amounts of deposits. In addition, within a given experiment, areas of vessels that had greater velocities, such as the center of the bottom of the beaker and along the plane of the impeller, had smaller amounts of deposits . Addai-Mensah[4] reported greater amounts of solid deposits in the dead zones, or zones of low shear, near baffles in the stirred tanks.

Some observations indicate that the effects of fluid flow on solids deposition are not simple. For instance, Mattus, et al.[5] (see Fig. 1) and Rosencrance et al.[3] both "reported observing swirl patterns and the formation of. "shark-teeth" deposits on the surfaces of test beakers, under conditions of low to moderate energy dissipation. The deposits formed under these conditions were held tenaciously on the metal surfaces.

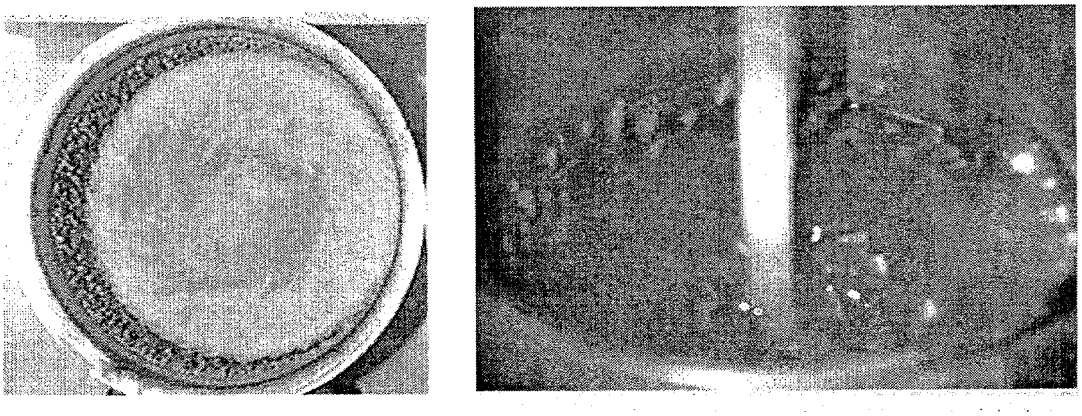

Fig. 1. Photographs of solids deposited in batch tests under low to moderate flow. Left: beaker after test, showing swirl pattern; right: "shark-teeth" deposits being formed during test.
Source: A. J. Mattus et al. (ref 5).

In addition, in our previous solids-deposition tests,' significant differences were observed in the amount and nature of solids deposited under quiescent and stirred conditions. Figure 2 shows results from the bottom side of a stainless steel foil sample during a stirred test. Notable in these images are the observations that significantly more solids were present on the bottom sides of the foils in the stirred tests than in the quiescent tests and that these solids were distributed in patterns that were similar to the top sides of the foils. The deposited solids on the foil surfaces were distributed in a "galaxy" pattern, apparently related to the fluid flow in the vessel. Some

areas were coated with a thin, translucent solids layer, while other areas were covered with macroscopic rough, particle deposits. The deposited solids more strongly adhered to the foil than those that were formed by settling in the quiescent tests. Scanning electron microscopy (SEM) images of the solids from the two areas showed different microstructures-the translucent layers are characteristic of heterogeneous growth of the solid film, while the macroscopic chunky solids appear to be the result of flow-induced deposition.

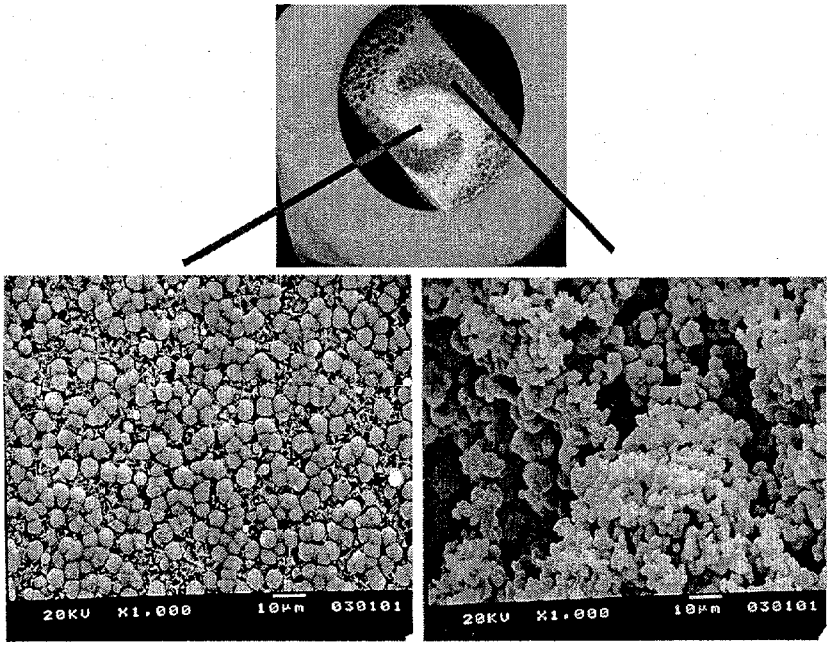

Fig. 2: Images from batch deposition tests, showing a significant effect of fluid flow on solids deposition. Top: Photograph of the lower surface of a metal foil after the test, showing a spiral pattern of macroscopic deposits in a field of translucent film. Bottom left: SEM image of translucent film, which is similar to that of the quiescent test and indicative of surface growth. Bottom right: SEM image of deposited solids. *Source:* Hu et al. (ref. 1).

3.2 LITERATURE REVIEW OF FLOW EFFECTS ON SOLIDS DEPOSITION

Particle formation, aggregation, and deposition-phenomena that occurred in the 2H evaporator during scale formation-involve complicated, interrelated processes. At the high electrolyte concentrations of the waste, electrostatic repulsion forces are neutralized and a net attractive force exists, resulting in a tendency for particle aggregation to occur. It is known from the literature (as discussed below) that the kinematics of fluid flow (or shear) affects 'particle-particle and particle-surface interactions and thus the phenomena of particle aggregation in solution and particle deposition onto solid surfaces. These are discussed briefly below.

Hydrodynamic Flow/Shear Effect on Particle Aggregation/Coagulation: The characteristics of particles (i.e., size, size distribution, density, surface roughness, hardness/softness, and concentration of the particles) in the bulk solution directly relate to the behavior and kinetics of particle deposition. Hydrodynamics significantly affects some characteristics of the particles and thus, particle deposition on surfaces.

Increased mixing (flow velocity or shear) in a stirred tank can promote collisions between particles. However, if the agitation is too vigorous, turbulent shear forces can break the aggregates into smaller aggregates and/or primary particles. It is not a simple task to determine the point at which agitation or shear leads to net breakup. Collisions among particles suspended in a turbulent flow may follow different mechanisms. Mutual approach of particles can be caused by local velocity gradients and by differing inertial response to the motion of the fluid. If turbulence is sufficient, particles may also collide after being transported from parts of the fluid that are uncorrelated with respect to fluid velocity. Whether or not the particles remain attached to one another after a collision is dependent on the net interparticle forces.

Several theoretical/modeling studies address particle coagulation by prediction of collision efficiency.[6-10] Smoluchowski[11] analyzed the effect of shear by deriving an equation for the collision rate of particles of uniform size in a simple laminar shear field. Its basic concept can also be applied to the description of collisions at the smallest scales of turbulence. Higashitani et al.[12] and Greene et al." used trajectory analysis to understand the effect of hydrodynamic and nonhydrodynamic forces on colloidal stability and shear coagulation for particles in a viscous fluid. Their analyses showed that the collision efficiency is higher in simple shear flow than in uniaxial extensional flow. Simulation results by Torres et al.[10] confirmed that shear can produce flocs with structures similar to Brownian aggregates.

Serra et al.[13,14] carried out experimental studies in a Couette-flow system to investigate aggregation and breakup of particles under laminar flow conditions. They identified three different regimes, depending on both the shear rate and the particle concentration. When the concentration is less than a critical value, the final diameter of the aggregate is independent of concentration and depends only on the shear. When the concentration is higher, two new regimes (corresponding to the transition from laminar to turbulent flow) are identified, with the final diameter of the aggregate depending on both the shear rate and the particle concentration. Serra and coworkers found that the flow between the cylinders became unstable when the shear rate was too low (0.51 s^{-1}) (transition from the laminar to turbulent flow regime is expected to be at a shear rate of 0.58 s^{-1}). The aggregation caused by Brownian motion can be neglected compared with the shear-induced aggregation when the Peclet number (Pe) = $6\pi\eta Gr^3/kT) > 129$, where η is the dynamic viscosity, G is the shear rate, r is the particle radius, k is the Boltzmann constant, and T is the temperature. When Brownian motion of the particles is unimportant, an analysis of aggregation reduces to determining particle trajectories," taking into account hydrodynamic interactions and nonhydrodynamic/physicochemical forces [e.g., attractive van der Waals and mostly repulsive electrical-double-layer (EDL) colloidal interactions] between the particles.

For a stirred tank equipped with a standard Rushton-turbine impeller, de Boer et al.[15] studied the effects of turbulent flow on particle coagulation. Several major findings are as follows. (1) At a low volume fraction of solid particles (-1 μm), the initial coagulation rates could be correlated with the average shear rate, as can be done for coagulation in laminar flow. (2) Coagulation rates in tanks of different sizes can be correlated with the specific power input. (3) The rate of growth for aggregates (l-20 μm) is approximately proportional to the cube root of the average rate of

shear in the tank. (4) The coagulation rate is approximately proportional to the square of the volume fraction of solids.

Hydrodynamic Flow/Shear Effect on Particle Adsorption/Deposition: Adsorption and deposition of particles from solution onto a solid surface must be considered in order to understand deposit formation on wall surfaces inside the 2H evaporator and gravity drain lines, although heterogeneous crystal growth from surface sites may be also responsible for formation of solid deposits. From the preceding discussion, we clearly see that the hydrodynamics (flow or shear) significantly affects the particle coagulation kinetics and equilibrium states as well as the final characteristics of particles in the bulk solution. The characteristics of particles directly affect the adsorption/deposition phenomena. Therefore, we can reason that the hydrodynamics of the suspension play a significant role in particle deposition.

The particle adsorption or deposition process can be regarded as the limiting case of the heterocoagulation,[16] and thus the particle-surface interaction energy can be described by the Derjaguin-Landau-Verwey-Overbeek (DLVO) theory, which is a static approach to describe the colloid-surface equilibrium system. In particular, Adamczyk and Weronski[17] have provided an excellent review of the application 'of the DLVO theory to problems associated with colloid particle adsorption and deposition at solid/liquid interfaces. A recent description of DLVO interaction energy between spheroidal particles and a flat surface is given by Bhattacharjee et al.[18] In the deposition process for charged particles onto oppositely charged surfaces, effects of ionic strength and size polydispersity of the particle suspension on diffusional deposition of colloidal particles were discussed by Semmler et al. The ionic strength (relating to the electrolyte concentration) defines the magnitude of the electrostatic repulsion between the particles, which in turn modifies the maximum surface coverage. The maximum surface coverage decreases with decreasing ionic strength. Particle size polydispersity also strongly influences the deposition process-small particles may fill voids left by larger particles such that the maximum surface coverage increases significantly. In a real dynamic deposition process, the size distribution of the deposited particles on the surface changes with time, whereby the small particles are adsorbed preferentially. Instead of the DLVO theory, Senger and coworkers[20] introduced the concept of *available surface function* and utilized statistical-geometrical approaches [i.e., Random Sequential Adsorption (RSA) and Ballistic Deposition (BD) models] and diffusional models for analyzing irreversible adsorption/deposition of colloidal particles on solid substrates.

In reality, particles dispersed in a fluid medium are subject to Brownian motion, external macroscopic flow, and/or microscopic flow. Using a similar classification of origins for particle coagulation,[12] we may classify particle-surface interactions as follows: *Brownian motion* is important for particles with diameters smaller than 1 μm, *shear stress* is important in the range of 1–40 μm, and *differential settling* is important for particles larger than 40 ym. Several studies[16,21,22] have amply demonstrated that particle deposition onto a surface is critically influenced by physicochemical as well as hydrodynamic parameters, which include particle size, size distribution, particle shape, particle density, hydrodynamic intensity, and the strength of van der Waals and EDL interaction fields.

Two hydrodynamic effects seem to be decisive: (1) transport of particles over macroscopic distances (convection) toward solid/liquid interfaces, where they become subject to specific force fields, and (2) microscopic scale coupling between local shearing flows and electrostatic repulsive interactions, leading to enhanced surface blocking (often referred to as "hydrodynamic scattering"). Warszynski[15] has shown that in the case of particles immersed in a polar medium, the effect of the electric field should already be considered at the stage of formulation of the equation describing motion of the fluid around particles. That leads to the electrokinetics effects such as electroviscous (or electrokinetic) drag or electrokinetic lift, which may influence adsorption of colloid particles at interfaces. The electrokinetic lift force (in the direction normal to the wall) appears when the charged particle moves along the charged wall. The coupling between hydrodynamics and electric interactions directly determines the rate of colloidal particle adsorption. At the beginning stage of particle deposition, when the surface is not covered by particles, strong fluid flow enhances the effect of attractive EDL forces between oppositely charged particles and surfaces, increasing the deposition rate. At later stages, when the surface is already partially covered by deposited particles, the repulsive EDL forces between adsorbed and adsorbing particles enhance the effect of "hydrodynamic" shadowing and thus considerably decrease the adsorption rate.

Any flow near the solid/liquid interface can be decomposed in local Cartesian coordinates into a stagnation point flow and a simple shear flow.[21] The hydrodynamic effect may thus be simplified into two scenarios by considering the shear effect (flow field parallel to the surface) and impinging flow effect (flow field perpendicular to the surface). In literature, impinging jet flow ("stagnant-point flow") has been particularly useful for theoretical studies as well as used popularly as a powerful technique in many experimental studies for directly measuring colloidal particle adsorption/deposition onto difference surfaces[16,21,22].

The deposition of particles onto a solid surface by an' impinging flow involves complicated processes, which are usually controlled by the simultaneous influence of convection, diffusion, colloidal and hydrodynamic interactions, and external body forces such as gravity. A deposition process can be conceptually divided into four stages: (1) particle transport in the bulk fluid, (2) displacement of the fluid between the particle and the surface, (3) particle interaction with surface by colloidal forces (van der Waals and EDL), and (4) stochastic effect when a particle is close to contacting the surface (discrete surface charges, surface heterogeneity and roughness). Yang et al.[22] have analyzed the kinetics of particle transport for a solid surface from an impinging jet under surface and external force fields. They have presented the influences of gravity, van der Waals, and EDL interactions on the particle deposition rates (in terms of the Sherwood number). They have found that asymmetric EDL interaction has an impact on the particle deposition rate and that the Sherwood number is strongly dependent on the characteristics of the energy profiles for the particle-surface interactions, such as the height of the energy barrier and the depth of the secondary energy minimum.

4. EXPERIMENTAL APPROACHES

Batch tests of two types were conducted: rheometer tests and stirred-tank flow tests. Testing of both types was limited to one set of conditions: a solution temperature of 80°C and initial overall 1:1 ratio of [Al] to [Si] at 0.133 *M.* The intensity of flow was the only parameter explored.

4.1 RHEOMETER TESTS

In these tests, a temperature-controlled rheometer with stainless steel wetted surfaces was used to measure solids deposition from simulant solutions under well-defined shear conditions. The weight of solids deposited on the spindle of the rheometer under various shear rates after a controlled, reaction time was measured. Because of the geometry of the system and the well-controlled shear provided by the rheometer, the shear in the sample cell is nearly homogeneous throughout the volume of fluid in proximity to the majority of the surface area of the spindle. This is in contrast to widely varying energy dissipation levels throughout a stirred tank. Therefore, the relationship between measured solids deposition and spindle rotational speed should provide a more reliable value for targeting local energy dissipation and fluid velocities near surfaces in the evaporator.

The experiments were conducted using a Brookfield DV-III rheometer with a temperature-controlled stainless steel cup and stainless steel spindle (type ULA). The procedure for the experiments is summarized in Table 1 and is detailed in Appendix A. The solutions were prepared as described in Appendix B. The solutions were preheated to 80°C in capped polyethylene containers in an oven and were filtered using 20-nm polytetrafluoroethylene (PTFE) syringe disk filters (Anotop 25 plus, Cat. No. 6809-4002, Whatman International Ltd.) prior to use. Aliquots of the preheated filtered solutions were mixed in the rheometer cup. The rheometer spindle was then placed in the solution and activated at the desired shear rate. The rheometer was held at constant temperature and shear rate for 2 h. The spindle of the rheometer was then removed from the solution and taken through a sequence of drying, weighing, and washing aimed at separating the mass of the material deposited on the side of the spindle from that settled on the top of the spindle and from salts of the simulant. It was determined that more-reproducible results were obtained by drying the spindle immediately and then rinsing off the salt from the solution, rather than immediately rinsing, which caused some of, the deposits to fall off the spindle. The implications of this finding are not known. The rheometer cup and spindle were cleaned with nitric acid before the next run.

Table 1. Summary of rheometer test procedure

1. Preheated, filtered (0.02 μm) Al and Si solutions separated
2. Solutions transferred to preheated rheometer cup
   - 0.133 *M* Si, 0.133 *M* Al overall; total volume: 16.2 mL
3. Cleaned, weighed stainless steel spindle immersed in solution, rheometer operated at 80°C at desired rpm for 2 h
   - Deionized water added every 30 min to reduce effect of evaporation
4. Spindle carefully removed from solution, placed in oven at 80°C for 1 h
   - Yields masses of deposit on sides + deposits on top + spindle + salt from solution
5. Spindle dipped gently (just below the top level) in three beakers of deionized water and then dried
   - Yields masses of deposit on sides + deposits on top + spindle
6. Spindle dipped (just below the top level) in beaker of 6 *M* HN03 for 30 s, and then dried
   - Yields masses of deposits on top + spindle
   - Difference is mass of deposits on sides

Tests conducted at low rotational speed indicated that the 16.2-mL total solution volume and a 2-h reaction time would allow a measurable and relatively reproducible amount of deposit to form. Subsequent tests were thus conducted under those conditions. The rheometer can be operated at rotational rates in the range 0.01 to 250 rpm, delivering shear rates in the range 0.012 to 306 s^{-1} for the spindle that will be used initially. (Other shear rates are possible using other spindles.) Initial testing was performed at five rotational speeds: 1, 10, 50, 100, and 250 rpm, with triplicate readings collected at 1, 10, and 100 rpm. These rates will bracket the shear rates in the majority of the evaporator system, with the possible exception of the vicinity of the steam lance outlet (The shear rate in the lift line and gravity drain lines are estimated to be on the order of 16 s^{-1}.) The conditions of subsequent testing were determined by the obtained results to concentrate points in the level of shear over which the measured deposition rate varies greatly.

4.2 STIRRED-TANK FLOW TESTS

A set of batch-type tests was conducted using a stirred tank containing solution that is recirculated through sections of stainless steel tubing (Fig. 3). The experimental setup is similar to those of Rosencrance[3] and Mattus,[5] with the addition of the recirculation loops. The tests were conducted to measure the effect of flow rate on the amount of solids deposited inside the sections of stainless steel tubing incorporated in the recirculation loops. These tests were designed to provide additional information on the relationship of shear to deposition to verify and augment results obtained in the rheometer tests. In addition, these tests have relevance to flow in the lift.. and gravity drain lines and are designed to determine the minimum flow rate needed to reduce deposition.

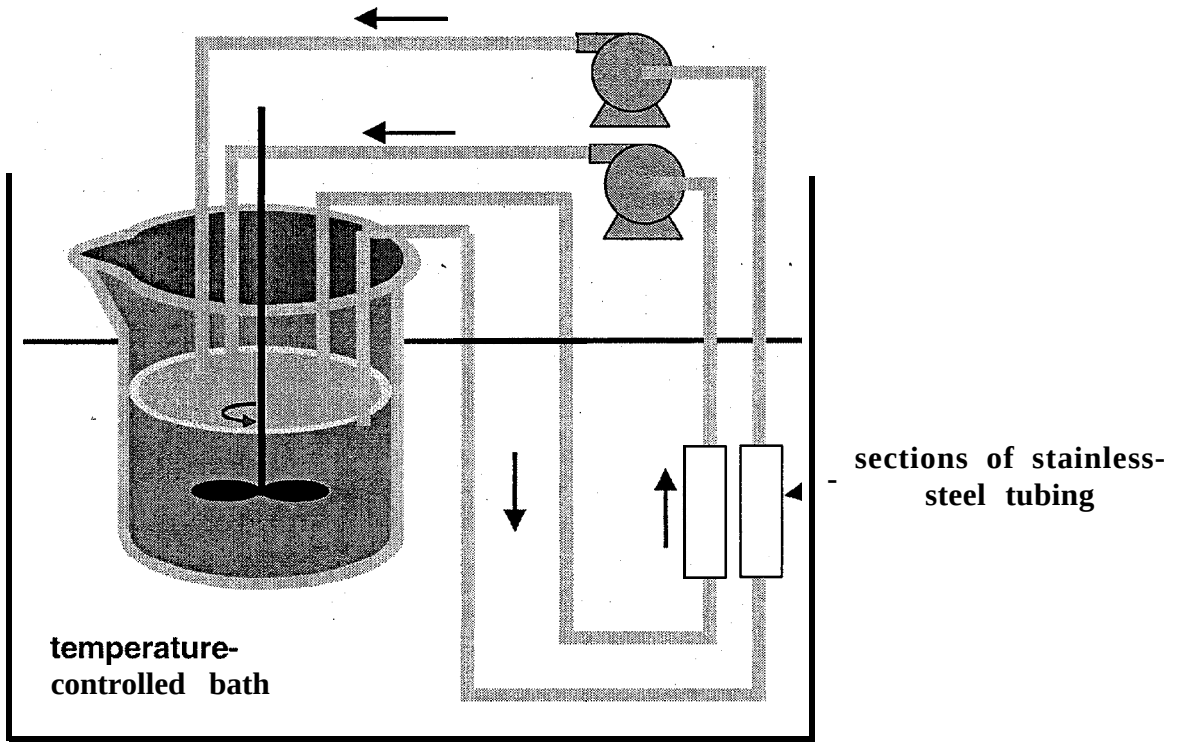

Fig. 3. Schematic of setup for stirred-tank flow test.

Sample streams were drawn from the beaker and flowed through 1/8-in. PTFE lines through samples of stainless steel tubing that sealed in the line using PTFE tubing fittings and were immersed in the water bath to hold them at temperature. Digital gear pumps (pump Model GA-T23, Micropump, Inc.) were used to generate smooth flow in the range of 6-360 mL/min; the pumps were placed downstream of the stainless steel samples to minimize the shear effect of the pumps.

The experiments were conducted at 80°C and a 1: 1 ratio of [Al] to [Si]. The procedure for the experiments is summarized in Table 2. Solutions were prepared as described in Appendix B. The solutions were not filtered prior to the experiment. The solutions were to be preheated to 80°C and then added in the desired proportion to the reaction beaker, with a total volume of 400 mL. As described in the results section, in several tests the reactive starting solution'was not fully at 80°C, which caused distinctly different solids deposition. The solution was stirred at 300 rpm using a Lightnin mixer and a polyethylene impeller, conditions that were shown by Rosencrance[3] to minimizes deposition in the beaker. Preweighed stainless steel tubing samples were placed in the recirculation lines, and the recirculation pumps were activated at the desired flow rates. The experiments were held at constant temperature, stirring, and recirculation flow rate for 2 h. The stainless steel tubing samples were removed from the lines, cleaned by dipping in distilled water

several times, and then dried by heating in an oven at 80°C. The mass of the solid deposit was determined by the difference of the mass of the dried tube and the weight of the tube after rinsing with nitric acid and drying.

Table 2. Summary of flow test procedure

1. Preheated Al and Si solutions separated
2. Solutions transferred to stainless steel beaker in water bath
   - 0.133 it4 Si, 0.133 *M* Al overall; total volume: 400 mL
3. Solution stirred at 300 rpm
4. Solution recycled through sections of stainless steel tubing
   - 1/8-in. PTFE tubing
   - 1/4- and 1/2-in. tubing, 1- and 2-in. lengths
5. Experiment run for 2 h
6. Tubing removed, rinsed with deionized water, and then dried in oven
   - Yields mass of tube + deposit
7. Tubing cleaned with 4 *M* nitric acid and then dried
   - Yields mass of tube; mass of deposit from difference

5. RESULTS

In both types of tests, it was noted that the fluid became turbid after only a few minutes. This indicates that the particle-forming reactions in bulk solution were rapid. Reaction kinetic data collected by Mattus et al.[2] also show that the concentrations of silicon and aluminum decrease quickly with time due to the solid particle formation. It would be expected that homogeneous growth in solution would be favored over heterogeneous growth directly onto the steel surfaces under these high-concentration conditions.

5.1 RHEOMETER TESTS

Photographs of spindles coated with solids from the rheometer tests are shown in Fig. 4. The amounts and characteristics of the solids varied visibly with shear rate. At low shear rates, the deposits were distributed throughout the surfaces of the spindle as a relatively even film, with some vertical gradient (see third image in Fig. 4). At higher shear rates, the solids formed in islands, with smaller amounts being deposited as shear rate was increased.

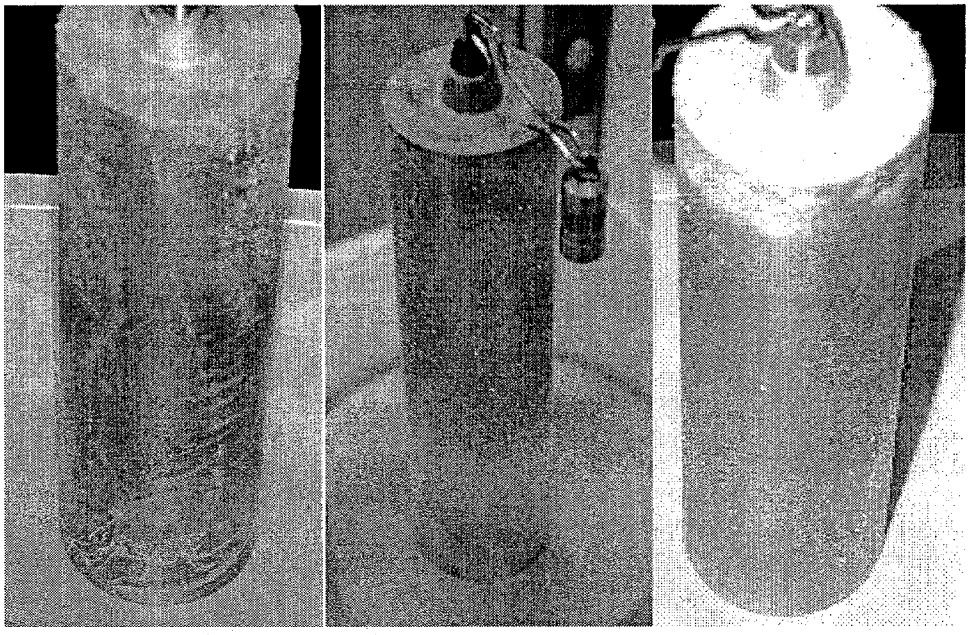

Fig. 4. Photographs of rheometer spindle after deposition tests: From left: (a) "smeared" deposit showing effect of contact with the rheometer cup when spindle was removed from solution (procedure was adapted to ensure consistent removal); (b) spindle from 10 rpm test showing concentration of deposit near bottom of spindle, (c) spindle from 50 rpm test showing light, even coverage of deposit and settled solids on top surface of spindle.

Results for these experiments are shown in Fig. 5. This figure presents three types of measurement data-(l) mass of all solids, including dried salt from the solution, the solids that settled on the top of the spindle, and the solids of interest on the sides of the spindle; (2) mass of solids on the top and sides, after rinsing the salt; and (3) mass of solids on the sides, after subtraction of the mass of the solids that settled on the top. It is apparent that a significant mass of solids settled on the top of the spindles; this mass was much larger than the amount that deposited on the sides of the spindles. Under these test conditions, the mass of solids deposited on the sides of the spindle was typically less than 50 mg, while the settled solids could be as much as five times that amount. Significant scatter is also notable in the results; multiple factors contributed to this scatter, including difficulties in removing the spindle from the cup, and rinsing the spindles without disturbing the solids and possibly inconsistent cleaning of the surfaces. After an initial increase at a low-rpm regime (c-10 rpm), the overall trend in Fig. 5 appears to be a reduction in the mass of solids with increased rotation rate.

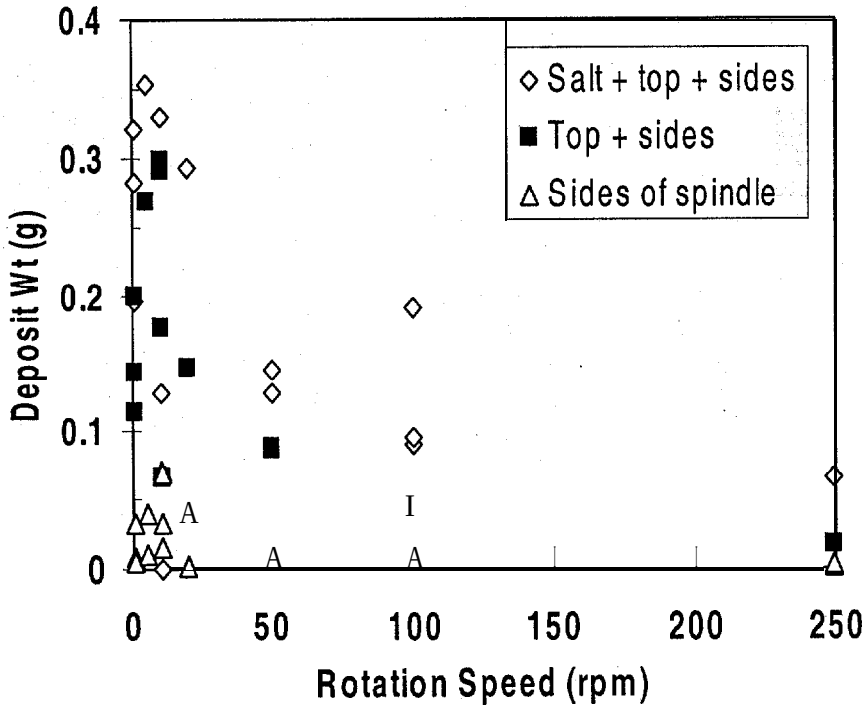

Fig. 5. Mass measurements from rheometer tests. The triangles denote the mass of solids deposited on the sides of the spindle, while the diamonds and solid squares indicate other solids on the spindle in intermediate steps.

The results obtained for the mass of solids deposited on the sides of the spindle are shown in Table 3, and the averages of the data are shown in Fig. 6.

Table 3. Rheometer test results

Rotation rate (rpm)	Shear rate (s^{-1})	Mass of deposited solids (g)
1	1.2	0.0329, 0.0087, 0.0045
5	6	0.0406, 0.0113
10	12	0.0700, 0.0702, 0.0327, 0.0160
20	24	0.0013, 0.0414
50	60	0.0082
100	120	0.0057, 0.0030, 0.0158, 0.0035, 0.0074
250’	300	0.0010, 0.0036

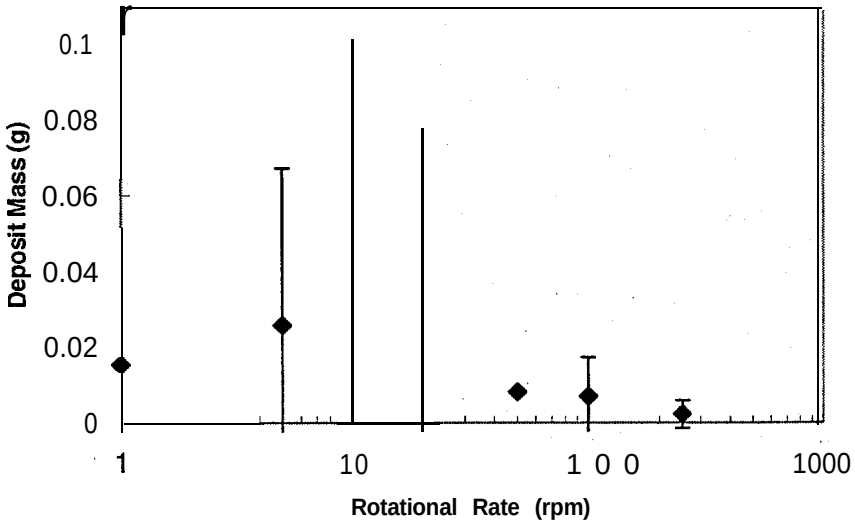

Fig. 6. Results of rheometer tests presented as averages of data for each rotational rate. Error bars denote 95% confidence intervals on multiple measurements.

The scatter of the data in Table 3 suggests that solid deposition is very sensitive to the test conditions. The average results presented in Fig. 6 show a trend of deposition with shear rate. A maximum quantity of solids deposition occurred at 10 rpm (corresponding to shear rate = 12 s^{-1}). Both below and above that rate, smaller amounts of solids were deposited, while there is a steep variation of deposition with rotational rate in the vicinity of the maximum. This trend is not statistically significant at the 95% confidence interval, indicating that further testing is warranted if agitation is identified as a primary means of mitigating solids deposition.

5.2. STIRRED-TANK FLOW TESTS

Operationally, the flow tests were difficult to perform smoothly. The initial test setups that placed the stainless steel tubing horizontally and the gear pumps above the beaker did not maintain flow throughout the test, primarily due to particle settling and priming of the pumps. With tubes secured vertically and with the pumps positioned at the level of the beaker, it was possible to maintain flow throughout the tests.

Figure 7 shows typical results for solids deposited during tests in which flow was maintained. In these tests, a light film of solids was deposited throughout the inner surface of the tubing. The walls of the agitated beakers were also only lightly covered with deposits, similar to the results of other tests[2,3,5]. The majority of the solids were not attached to surfaces and settled to the bottom of the beaker with no agitation. The overall mass of the deposits on the inner walls of the tubes was typically less than 20 mg, with significant scatter in the measured mass of solids. The possible total mass of solids that could be produced in the experiments was approximately 8.8g. Figure 8 compares tubes that were run in the same experiment at the same flow rate; the difference appears to be that the tube with greater deposits (52 mg vs 11 mg) was held at an angle from vertical. This set of experiments yielded good qualitative data. However, because of

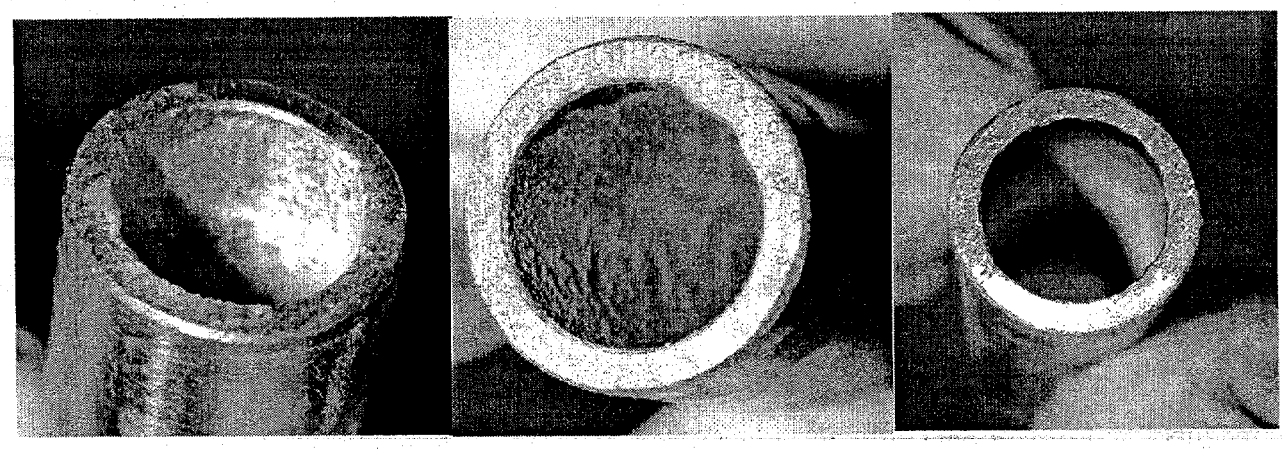

Fig. 7. Photographs of solids deposited during tests in which flow was maintained throughout the 2-h experiment.

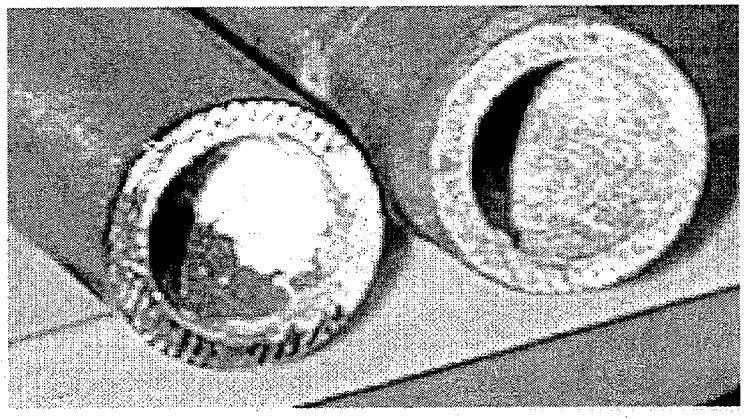

Fig. 8. Photograph of tubes showing settling effect. The ¼-in. tubes were run in the same experiment under matching conditions of flow rate. The left tube (deposit mass = 52 mg) appears to have been held at an angle, while the right tube (deposit mass = 11 mg) appears to have been held near vertical.

the low mass values, the scatter in the data, and small amount of flow rates for which flow was maintained, few quantitative trends can be deduced from the results.

Very striking results are presented in Fig. 9, which shows photographs of tubes that were fully clogged by deposits. In that case, the solution was poured into the beaker at room temperature, and pumped through the tubes at 34°C for 2 h, before a problem with the equipment was noted and the solution temperature was raised to 80°C. During the 2 h that the solution temperature was raised to 80°C, flow was essentially stopped by the plugging. In examining the conditions of experiments that resulted in plugged tubes, in every case the solutions were not fully preheated to 80°C when flow was initiated. The drastically different results of Fig. 7 and Fig. 9

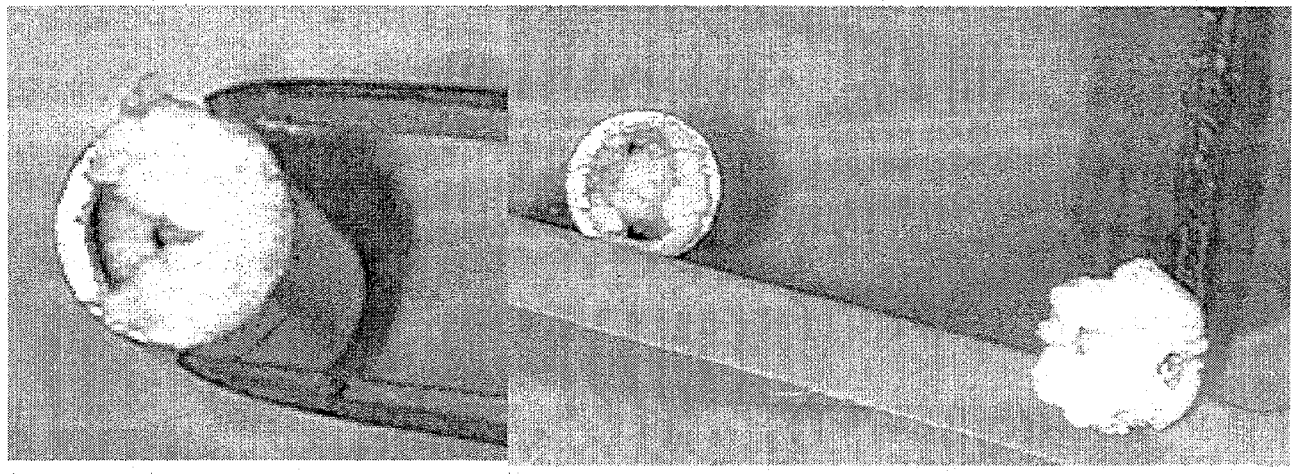

Fig. 9. Photographs of tubes that were fully clogged by deposits. In the experiment that produced these tubes, the solution was successfully pumped through the tubes at 34°C for 2 h before the temperature of the solution was raised to 80°C. Deposit masses in tubes shown in right image are 0.202g in 1.5-cm section (left) and 0.328g in 3-cm section (right).

indicate that a significant difference is found in the tendency of solids to deposit when they are held at 80°C and when they are mixed at a lower temperature and the solution is brought to 80°C. This appears to be a significant result that could be related to the scaling problems in the 2H evaporator and that warrants further investigation.

5.3 DISCUSSION OF RESULTS

The goals of this work were to

- confirm the importance of fluid flow on solids deposition,
- identify a target level for local energy dissipation and/or fluid velocity in the evaporator, and
- identify target levels for shear/velocity for flow in tubes, which relates to flow rates in the lift and gravity drain lines.

The rheometer tests addressed these objectives for the limited conditions studied. Those tests indicated that solids deposition is affected by fluid flow. Because maximum solids deposition in the rheometer tests was measured to occur at a shear rate of approximately 12 s^{-1}, a target level of energy dissipation in the evaporator would be one that would provide a shear rate near all surfaces significantly greater than 12 s^{-1}. Regarding flow in tubes, a 6 gal/min single-phase liquid flow through the 2-in. lift or gravity drain lines would result in a shear rate of approximately 16 s^{-1}; therefore, common operating conditions are not greatly above the shear rate that produced the maximum solids deposition in our simulant tests at 80°C.

Although the single set of experimental conditions does not match the conditions of evaporator operation [e.g., 80°C vs 120°C (and higher), substantially elevated silicon and aluminum concentrations], it is significant to the operation of the evaporator that the shear rate of maximum

solids deposition in the rheometer tests is in the range of realistic shear for portions of the system. These findings are consistent with those of Rosencrance et al.,[3] who found a significant reduction in deposition with increasing mixing rate under conditions with unknown, but relatively high shear rates near the walls. Shear rates near the interior surfaces of the 2H evaporator are likely to vary widely because of the complicated geometry and the nonuniform flows, and it is likely that significant areas will not have elevated shear. In addition, it appears that it would be very difficult to implement a means of agitation/mixing that would guarantee that all surfaces would greatly exceed 12 s^{-1}. Because of these issues, while it is likely that enhanced mixing will improve the situation, it does not appear advisable to depend on increased agitation as the primary means for reduction of scale in the 2H evaporator.

It is perhaps more significant that the tubes used in the flow tests became clogged with solids when the solutions were below 80°C at the start of the test. This is a very striking difference from experiments with fully preheated solutions, which yielded only thin films of solids on the tubes. These results suggest that there are significant differences in the "stickiness" of solids formed at different temperatures. If this can be verified, it may provide opportunities for engineering approaches to reduce solids deposition, such as (1) feed dispersion, which would be aimed at allowing the feed to reach evaporator temperature more quickly (to reduce the amount of time that amorphous sodium aluminosilicates would be present), or (2) feed preheating, possibly through combining with a recycled stream of evaporator effluent.

Based on the results of these experiments, the following tests are recommended:

- Further rheometer studies at lower aluminum and silicon concentrations (possibly with continuous flow to build up measurable and less-fluctuating data concerning the mass of solids on the surfaces of rheometer spindle). These tests would have value in determining if the results obtained here are characteristic of all concentrations. It is likely that the effects of shear will be different at some lower concentration, since heterogeneous growth directly on surfaces will be favored as the concentration of aluminum and/or silicon is decreased.
- Studies to determine which forms of sodium aluminosilicates adhere to stainless steel surfaces, under what conditions these materials are created, and what viable approaches are available for plant operations to avoid the creation of those "sticky" forms.

6. REFERENCES

1. Hu, M. Z.-C., D. W. DePaoli, and D. T. Bostick, *Dynamic Particle Growth Testing-Phase I Studies,* ORNL/TM-2001/100, Oak Ridge National Laboratory, July 2001.

2. Mattus, A. J., C. H. Mattus, and R. D. Hunt, *Kinetic Testing of Nitrate-Based Sodalite Formation over the Temperature Range* of 40 *to 100°C*, ORNL/TM-2001/117, Oak Ridge National Laboratory, Oak Ridge, Tenn., August 2001.

3. Rosencrance, S. W., D. Herman, and D. Healy, *Formation and Deposition of Aluminosilicates in Support of the 2H Evaporator Fouling Program* (U), WSRC-TR-2001-00464, Westinghouse Savannah River Company, Aiken, S.C., September, 2001.

4. Addai-Mensah, J., *Sodium Aluminosilicate Scale Formation in Westinghouse Savannah River Company 2H Evaporation Process,* Report No. 1 of Westinghouse Savannah River Company subcontract AC18106S, Ian Wark Research Institute, University of South Australia, Mawson Lakes, Adelaide, Australia, May 18, 2001.

5. Mattus, A. J., Oak Ridge National Laboratory, Oak Ridge, Tenn., *Investigation Into the Control and Kinetics of Aluminosilicate Formation on Stainless Steel Surfaces at 100°C*, ORNL/TM-2002/47, Oak Ridge National Laboratory, Oak Ridge, Tenn., February 2002.

6. Tontrup, C. F. Gruy, and M. Cournil, *J. Colloid Interface Sci.,* **229**, 5 11 (2000).

7. Brunk, B. K., D. L. Koch, and L. W. Lion, *J. Fluid Mech.*, *364,* 81 (1998).

8. Kusters, K. A., J. G. Wijers, and K. Thoenes, *Chem. Eng.. Sci., 52,* 107 (1997).

9. Greene, M. R., D. A. Hammer, and W. L. Olbricht, *J. Colloid Interface Sci.,* 167,232 (1994).

10. Torres, F. E., W. B. Russel, and W. R. Schowalter, *J. Colloid Interface Sci.,* 145, 51 (1991).

11. Smoluchowski, M. Z., *Phys. Chem., 92,* 129 (1917)

12. Higashitani, K. R. Ogawa, and G. Hosokawa, *J. Chem. Eng. Jpn.,* 15,299 (1982)

13. Serra, T., J. Colomer, and X. Casamitjana, *J. Colloid Interface Sci.,* 187,466 (1997)

14. Serra, T. and X. Casamitjana, *J. Colloid Interface Sci., 206,505* (1998)

15. de Boer, G. B. J., G. F. M. Haedemakers, and D. Thoenes, *Chem. Eng. Res.* **67**, 3011 (1989)

16. Warszynski, P., *Adv. Colloid Interface Sci.,* **84**, 47 *(2000)*

17. Adamczyk, Z. and P. Weronski, *Adv. Colloid Interface Sci., 83,* 137 (1999).

18. Bhattacharjee, S., J. Y. Chen, and M. Elimelech, *Colloids Surf. A,* 165, 143 (2000).

19. Semmler, M., J. Ricka, and M. Borkovec, *Colloids Surf. A,* **165**, 79 (2000).

20. Senger, B., J.-C. Voegel, and P. Schaaf, *Colloids Surf: A,* 165,255 (2000).

21. Adamczyk, Z., P. Warszynski, L. Szyk-Warszynska, P. Weronski, *Colloids Surf.*, 165, 157 (2000).

22. Yang, C., T. Dabros, D. Li, J. Czamecki, and J. Masliyah, *J. Colloid Interface Sci. 208, 226* (1998).

Appendix A. PROCEDURE FOR RHEOMETER TESTING OF SOLIDS DEPOSITION FROM SRS SIMULANTS

1. Balance Calibration Check

Zero the Mettler AE 200 balance with the door closed. Using tweezers, sequentially place a l-, 10-, and 100-g weight from weight 15469 on the balance pan and determine its weight. After the weight is determined for each standard, also tare the balance to determine whether the tare works correctly at that weight. Enter data on the Balance Calibration Sheet. After removing the weight from the balance, rezero before the next weight standard is placed on the pan.

2. Rheometer Setup and Operation

A. Check that the water bath temperature is -82°C. The rheometer barrel should be cleaned with -4iV HNO_3, triply rinsed with deionized water, and dried. The spindle should be similarly cleaned. Check that the barrel and spindle do have not solid deposits on their surfaces. Place the spindle and a clean plastic weighing boat in the oven for 30 min while setting up the rheometer.

B. Open "Evaporator Rheometer Results Aug 01" spreadsheet; make a new data sheet and enter data pertaining to the experiment to be run.

C. Open Rheocalc Vl.l; check that the barrel temperature is 80°C. Zero the rheometer by pressing the zeroing icon. Once the instrument is zeroed, press the computer icon and then select the View/Edit Program and select the folder to retrieve the current program file "david.bvs." Use the AI icon to change the run speed of the spindle. Typical program time is 2 h. Enter a name for the data file.

D. Using gloves, remove the spindle and weighing dish from the oven and place them in the desiccator to cool for 10 min. Using gloves, place the spindle on weighing paper in the balance; enter the weight in the spreadsheet under the "Spindle Tare" value.

E. Using gloves, connect the spindle and check that it is concentrically aligned with the rheometer barrel. Filter 5.4 mL of heated SRS solution A and 10.8 mL of heated SRS solution B with 0.02-μm Acrodisc filters and pour sequentially into the barrel. Immediately lower the spindle into the barrel and tighten the alignment screw. Start the program by pressing the rocket icon.

F. Every 30 min, view the liquid level in the rheometer barrel using the dental mirror and light source. Add deionized water (usually three short squirts) to the side of the cup to bring the level to just above the top of the spindle.

G. When the run is completed, carefully remove the barrel so that it does not touch the sides of the spindle. Discard the barrel solution. While wearing gloves, disconnect the spindle, touching only the screw connector and hook. Place the spindle on the weighing boat and into the oven for 1 h. Determine the weight of the spindle at thispoint. Holding the spindle by the connector, dip it gently into three successive water rinses before placing it on the weighing boat. Place the boat and spindle in the drying oven for 30 min, taking care not to dislodge any deposits from the spindle. Remove the dish with spindle from the oven at the end of the drying time, and place it immediately in a desiccator for 10 min. Immediately weigh the spindle.

H. Holding the spindle by the connector, gently dip it in the 6 N HNO_3 bath and then in the three successive water rinses. Place the spindle on the weighing boat, and insert it into

the drying oven for 30 min. Remove the dish with spindle from the oven at the end of the drying time, and place it immediately in a desiccator for 10 min. Immediately weigh the spindle.

3. Preparation for Next Experiment

Rinse the spindle with 4 *N* HNO_3, and then with distilled water. Polish dry the surface with a Kimwipe before placing it in the oven for storage. Clean the rheometer barrel by rinsing twice with distilled water, once with 4 *N* HNO_3, and three times with distilled water. Use a Kimwipe to dry the barrel.

Appendix B. SOLUTION PREPARATION

Two types of solutions were prepared for these experiments-an aluminum-containing solution (A), and a silicon-containing solution (B).

Solution A was prepared by first dissolving solid NaOH in nanopure water in an open vessel to avoid pressurization due to the exothermic dissolution process. This operation was performed in a fume hood. Once the solution cooled to. room temperature, aluminum nitrate was added and dissolved. After complete dissolution of the aluminum salt, sodium nitrate was dissolved, followed by sodium nitrite. The final solutions were brought to volume with nanopure water, resulting in the following compositions:

	mol/L
NaOH	2.50
$NaNO_3$	3.00
$NaNO_2$	3.00
$Al(NO_3)_3 \cdot 9H_2O$	0.40
Total Na^+	8.50
Total OH^-	0.90
Total NO_3^-	4.2
Total NO_2^-	3.00
Total Al^{3+}	0.40

Solution B was prepared by dissolving 240 g of sodium hydroxide (EM Science) in 800 mL of deionized water in a 1200-mL stainless steel beaker. 'Twenty grams of SRS glass Frit 200 was then added; a Teflon-coated stirring bar was used to disperse the frit. A water-cooled condenser column was attached to a stainless steel top and used to cover the beaker during heating. The solution was boiled under reflux for up to 20 h. The cooled solution was filtered through a Whatman No. 1 paper filter into an open Nalgene 1-L volumetric flask and brought to 1000-mL volume with nanopure water, resulting in the following composition:

NaOH	6 *M*
Silica Frit 200	20 g/L
Si	0.2 M
Final OH-	5.53 M

When combined in a volume ratio of 1 part solution A to 2 parts solution B, the sample mixture contains the following:

	mol/L
Total Na^+	6.83
Free OH	3.99
Total NO_3	1.40
Total NO_2	1.00
Total Al^{3+}	0.133
Total Si	0.133

Appendix C. SUMMARY OF RHEOMETER TESTS

Date	rpm	Dry simulant wt (g)	Water rinse w. (g)	Acid rinse wt (g)	Dry acid wt (g)	Data file	Significant comments
8/27/01	1	0 NA	0.0780	0.0535	NA	2hsrsl 0a.dv3	Did not add water to maintain liquid level
8/28/01	1	0 NA	0.1810	0.0141	NA	2hsrs10b.dv3	Start adding water every 30 min to wet top of spindle
8/29/01	1	0 NA	0.0456	0.0370	NA	2hsrsl 0c.dv3	
		10 NA	0.0084	0.0052	NA	2hsrsl 0d.dv3	Spindle shaken in water baths
8/30/01	1	0 0.4408	0.2970	0.0702	0.3706	2hsrs10e.dv3	Start dipping spindle into three rinse beakers; not shaken
		10 0.3283	0.1762	0.0700	0.2583	2hsrs10f.dv3	First 15 min-cup not tightened fully, spindle rpm variable
8/31/01	1	0 NA	0.2909	0.0327		2hsrsl 0g.dv3	No simulant drying step
		100 0.0899	0.0449	0.0057	0.0842	2hsrs100a.dv3	Spectral post used to withdraw barrel from spindle at end of exp.; some material scraped off
		100				2hsrs100b.dv3	Material scraped from spindle; run not completed
9/1/01	1	0 0 0.1032	0.0610	0.0030	0.1002	2hsrs100c.dv3	New support used to hold cup while rheometer lifted by stand; back side of spindle rubbed on cup w/lifting
9/3/01	1	0 0 0.1847	0.1003	0.0158	0.1689	2hsrs100d.dv3	
9/4/01	1	0 0 0.0952	0.0661	0.0035	0.0916	52hsrs100e.dv3	Spectral post used to withdraw spindle at end of exp.
		100 0.1907	0.0558	0.0074	0.1833	2hsr100f.dv3	High (-4 cp) initial viscosity; took a little longer to insert and align spindle
		10 0.1286	0.0657	0.0160	0.1126	2hsr10g.dv3	Viscosity values very unstable around 20 min; nothing is loose; rotation and solution level look OK; steady when water was added
9/5/01		1 0.2827	0.1444	0.0087	0.2739	52hsrs1a.dv3	Spectral post used to withdraw barrel from spindle at end of exp.; spindle sticks on back side during withdrawal
		1 0.3197	0.1991	0.0329	0.2868	52hsrs1b.dv3	Spectral post used to withdraw barrel from spindle at end of exp.; spindle sticks on back side during withdrawal
9/6/01		1 0.1953	0.1138	0.0045	0.1908	2hsrs1c.dv3	Spectral post used to withdraw barrel from spindle at end of exp.; spindle sticks on back side during withdrawal
		50 0.1460	0.0883			2hsrs50a.dv3	Spectral post used to withdraw barrel from spindle at end of exp.; spindle sticks on back side during withdrawal
		50				2hsrs50b.dv3	Spectral post used to withdraw barrel from spindle at end of exp.; spindle sticks on back side during withdrawal

9/11/01	5	0.3539	0.2688	0.0113	0.18812hsr5b.dv3	Viscosity remains fairly steady throughout run; yesterday's 5-rpm run had above-scale excursions late in the run
	20	0.2935	0.1468	0.0414	0.09642hsr20b.dv3	Had a lot of trouble getting the barrel screw into position before experiment started
9/12/01	5 0	0.1273	0.0869	0.0082	0.04862hsrs50c.dv3	
	249	83.3098	0.0171	0.001	0.04922hsr249b.dv3	Viscosity values are over instrument range
9/7/01	2 4 9			0.0036	2hsr249a.dv3	Weight data on 9-7-01 and 9-l O-01 lost to computer crash
9/10/01	5			0.0406	2hsrs5a.dv3	Weight data on 9-7-01 and 9-10-01 lost to computer crash
	20			0.0013	2hsrs20a.dv3	Weight data on 9-7-01 and g-10-01 lost to computer crash

INTERNAL DISTRIBUTION

1. V. F. de Almeida
2-6. D. T. Bostick
7-11. D. W. DePaoli
12. J. N. Herndon
13-17. M. Z. Hu
18. R. D. Hunt
19. A. J. Mattus
20. C. P. McGinnis
21. S. M. Robinson
22. C. Tsouris
23. A. B. Walker
24. J. S. Watson
25. C. Weber
26. T. D. Welch
27. Central Research Library
28. ORNL Laboratory Records-RC
29.-30. ORNL Laboratory Records-OSTI

EXTERNAL DISTRIBUTION

3 1. C. S. Boley, Westinghouse Savannah River Company, Building 703-H, Room 137, Aiken, SC 29808

32. T. E. Britt, Westinghouse Savannah River Company, Building 703-H, Room 85, Aiken, SC 29808

33. T. M. Brouns, Pacific Northwest National Laboratory, P.O. Box 999, MS K9-91, Richland, WA 99352

34. L. D. Bustard, Sandia National Laboratories, P.O. Box 5800, MS: 0728, Albuquerque, NM 87185-5800

35. B. Carteret, Pacific Northwest National Laboratory, P.O. Box 999, MS K9-91, Richland, WA 99352

36. E. J. Cruz, U.S. Department of Energy, Richland Operations Office, P.O. Box 550, MSIN: H6-60, Richland, WA 99352

37. R. E. Edwards, Westinghouse Savannah River Company, Building 704-3N, Aiken, SC 29808

38. P. D. d'Entremont, Westinghouse Savannah River Company, Building 703-H, Room 97, Aiken, SC 29808

39. Kurt Gerdes, Tanks Focus Area Headquarters Program Lead, DOE Office of Science and Technology, 19901 Germantown Rd., 1154 Cloverleaf Building, Germantown, MD 20874-1290

40. P. W. Gibbons, Numatec Hanford Corporation, P.O. Box 1970, MS: H5-61, Richland, WA 99352

41. R. L. Gilchrist, Pacific Northwest National Laboratory, P.O. Box 999, MS: K9-91, Richland, WA 99352

42. T. S. Gutmann, U.S. Department of Energy, Savannah River Operations Office, P.O. Box A, Aiken, SC 29802

43. E. W. Holtzscheiter, Westinghouse Savannah River Company, Savannah River Technology Center, Building 773-A, Room A-229, MS: 28, Aiken, SC 29802

44. J. 0. Honeyman, Lockheed Martin Hanford Corporation, P.O. Box 1500, MS: G3-21, Richland, WA 99352

45. G. Josephson, Pacific Northwest National Laboratory, P.O. Box 999, MS: K9-91, Richland, WA 99352

46. B. L. Lewis, Westinghouse Savannah River Company, Building 703-H, Room 99, Aiken, SC 29808

47. K. A. Lockie, U.S. Department of Energy, Idaho Operations Office, 750 DOE Place, MS: 1145, Idaho Falls, ID 83402

48. J. P. Morin, Westinghouse Savannah River Company, Savannah River Technology Center, Building 703-H, Aiken, SC 29808

49. J. R. Noble-Dial, U.S. Department of Energy, Oak Ridge Operations Office, P.O. Box 2001, Oak Ridge, TN 37830-8620

50. J. F. Ortaldo, Westinghouse Savannah River Company, Building 704-S Room 13, Aiken SC 29808

5 1. Lynne Roeder-Smith, Tanks Focus Area Technical Team Communications, Pacific Northwest National Laboratory, P.O. Box 999, MSIN: K9-69, Richland, WA 99352

52. W. L. Tamosaitis, Savannah River Technology Center, Westinghouse Savannah River Company, Bldg. 773-A, Room A-23 1, Aiken, SC 29808

53. M. T. Terry, Los Almos National Laboratory, P.O. Box 999, K9-69, Richland, WA 99352

54. T. R. Thomas, Lockheed Martin Idaho Technologies Company, P.O. Box 1625, MSIN: 3458, Idaho Falls, ID 83415-3423

55. J. H. Valentine, Bechtel BWXT Idaho, Inc., P.O. Box 1625, MS: 3211, Idaho Falls, ID 83415-3100

56. W. B. Van Pelt, Westinghouse Savannah River Company, Building 773-42A, Room 121, Aiken, SC 29808

57. J. Westsin, Pacific Northwest National Laboratory, P.O. Box 999, MS: K9-91, Richland, WA 99352

58. W. R. Wilmarth, Westinghouse Savannah River Company, Building 773-42A, Room 153, Aiken, SC 29808

59. Tanks Focus Area Program Office, c/o T. Pietrok, U.S. Department of Energy, Richland Operations Office, P.O. Box 550, MS: K8-50, Richland, WA 99352

60. Tanks Focus Area Technical Team, c/o B. J. Williams, Pacific Northwest National Laboratory, P.O. Box 999, MSIN: K9-69, Richland, WA 99352